Journal of Fluorescence (2021) 31:1401–1407
https://doi.org/10.1007/s10895-021-02767-4

ORIGINAL ARTICLE

Lack of Environmental Sensitivity of a Naturally Occurring Fluorescent Analog of Cholesterol

Amitabha Chattopadhyay[1] · Samares C. Biswas[1] · Raju Rukmini[1] · Satyen Saha[2,3] · Anunay Samanta[2]

Received: 29 March 2021 / Accepted: 1 June 2021 / Published online: 5 July 2021

Abstract

Dehydroergosterol (DHE, $\Delta^{5,7,9(11),22}$-ergostatetraen-3β-ol) is a naturally occurring fluorescent analog of cholesterol found in yeast. Since DHE has been shown to faithfully mimic cholesterol in a large number of biophysical, biochemical, and cell biological studies, it is widely used to explore cholesterol organization, dynamics and trafficking in model and biological membranes. In this work, we show that DHE, in spite of its localization at the membrane interface, does not exhibit red edge excitation shift (REES) in model membranes, irrespective of the membrane phase. These results are reinforced by semi-empirical quantum chemical calculations of dipole moment changes of DHE in ground and excited states, which show a very small change in the dipole moment of DHE upon excitation. We conclude that DHE fluorescence exhibits lack of environmental sensitivity, despite its usefulness in monitoring cholesterol organization, dynamics and traffic in model and biological membranes.

Keywords DHE · REES · Excited state dipole moment · Membrane penetration depth · Fluorescent sterol

Introduction

Cholesterol is an essential and unique lipid in higher eukaryotic cellular membranes and plays a vital role in membrane organization, dynamics, function, and sorting [1–3]. A hallmark of the organization of membrane cholesterol is its nonrandom distribution in domains [4–6]. Membrane cholesterol has been recognized as a vital lipid in the function of crucial membrane proteins such as ion channels and receptors [7–14] and in the entry of intracellular pathogens to host cells [15]. Interestingly, cholesterol has been implicated in endocytosis and intracellular traffic of membrane receptors [16–19]. Intracellular cholesterol traffic among organelles helps to maintain cellular cholesterol homeostasis. Dysregulated cholesterol traffic in cells has been reported to give rise to serious and fatal neurological diseases such as Niemann-Pick type C [20].

Fluorescent sterols offer a powerful approach for monitoring cholesterol organization, dynamics and trafficking in membranes due to their high sensitivity, time resolution, and multiplicity of measureable parameters [21–24]. Naturally occurring fluorescent analogs have an advantage in this context, since they do not perturb the membrane as much as sterols that are covalently linked to external fluorophores (due to bulky and polar nature of the fluorescent group). Dehydroergosterol (DHE, $\Delta^{5,7,9(11),22}$-ergostatetraen-3β-ol) is a naturally occurring fluorescent analog of cholesterol which is found in yeast and differs from cholesterol in having three additional double bonds and a methyl group (see Fig. 1). A number of previous reports have shown that DHE faithfully mimics natural cholesterol in biophysical, biochemical, and cell biological studies [25–29]. For this reason, DHE has been extensively used to monitor cholesterol organization, dynamics and trafficking in model and cellular membranes [27, 30–34].

An important property of a fluorophore is its sensitivity to the microenvironment in which it is localized. This makes fluorescence an excellent marker of any change in fluorophore microenvironment by change in parameters such as emission maximum. However, all fluorophores do

✉ Amitabha Chattopadhyay
amit@ccmb.res.in

[1] CSIR-Centre for Cellular and Molecular Biology, Uppal Road, Hyderabad 500 007, India

[2] School of Chemistry, University of Hyderabad, Hyderabad 500 046, India

[3] Department of Chemistry, Banaras Hindu University, Varanasi 221 005, India

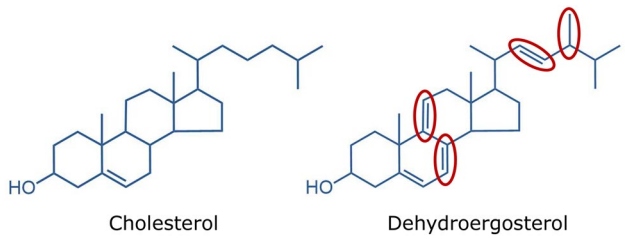

Fig. 1 Molecular structures of cholesterol (left) and the naturally occurring fluorescent cholesterol analog dehydroergosterol (DHE; right). DHE differs from cholesterol in three additional double bonds and a methyl group (highlighted in its chemical structure). DHE has been shown to faithfully mimic the properties of cholesterol in several biochemical, biophysical, and cell biological studies. See text for more details

not share this property. For example, although tryptophan, a naturally occurring fluorescent amino acid, is characterized by environment-sensitive fluorescence, tyrosine (another naturally occurring fluorescent amino acid) and serotonin (a tryptophan derivative which acts as a neurotransmitter) display lack of environmental sensitivity in their fluorescence [35, 36]. In this paper, we report that DHE does not exhibit red edge excitation shift (REES) in model membranes, irrespective of the membrane phase. These results are supported by semi-empirical quantum chemical calculations of dipole moment changes of DHE in ground and excited states. In other words, DHE fluorescence, although useful for monitoring cholesterol organization, dynamics and traffic in model and cell membranes, lacks environmental sensitivity.

Experimental

Materials

DHE, 1,2-dimyristoyl-*sn*-glycero-3-phosphocholine (DMPC), 3-(*N*-morpholino)propanesulfonic acid (MOPS), Na_2HPO_4 and NaCl were purchased from Sigma Chemical Co. (St. Louis, MO). 1,2-Dipalmitoyl-*sn*-glycero-3-phosphocholine (DPPC), 1-palmitoyl-2-oleoyl-*sn*-glycero-3-phosphocholine (POPC), 1-palmitoyl-2-(5-doxyl)stearoyl-*sn*-glycero-3-phosphocholine (5-PC), and 1-palmitoyl-2-(12-doxyl) stearoyl-*sn*-glycero-3-phosphocholine (12-PC) were obtained from Avanti Polar Lipids (Alabaster, AL). The anthroyloxy-labeled fatty acids, 2-(9-anthroyloxy)stearic acid (2-AS) and 12-(9-anthroyloxy)stearic acid (12-AS), were from Molecular Probes/Invitrogen (Eugene, OR). The concentration of DHE stock in methanol was determined by measuring absorbance utilizing a molar extinction coefficient (ε) of 10,500 M^{-1} cm^{-1} at 324 nm [37]. Purity of POPC and DPPC was checked by thin layer chromatography with a chloroform/methanol/water (65:35:5, v/v/v) mobile phase using silica gel pre-coated plates from Merck (Darmstadt, Germany). Both lipids gave one spot with a phosphate-sensitive spray and subsequent charring [38]. Phospholipid estimation was carried out by total digestion using perchloric acid, followed by a colorimetric phosphate assay using Na_2HPO_4 as standard [39]. DMPC was used as an internal standard to confirm complete lipid digestion. All other chemicals used were of the highest purity available. Spectroscopy grade solvents and water purified through a Millipore (Bedford, MA) Milli-Q system were used for all experiments.

Sample Preparation

Samples containing 320 nmol of POPC (or DPPC) and 16 nmol of DHE were dissolved in methanol and a few drops of chloroform and mixed well. Lipids were first dried while being warmed gently (~35 °C) under a stream of nitrogen, followed by further drying for at least 3 h under a high vacuum in order to remove the remaining traces of solvent. After complete drying, 1.5 ml of buffer (100 mM MOPS, 150 mM NaCl, pH 7.2) was added to the dried lipid film and vortexed for 3 min to ensure a homogeneous dispersion. During vesicle preparation, the buffer was maintained at a temperature well above the phase transition temperature of the constituent lipids. Large unilamellar vesicles (LUVs) of 100 nm diameter were prepared using an Avestin Liposofast Extruder (Ottawa, Canada) by the extrusion method, as described previously [32]. Briefly, multilamellar vesicles (MLVs) formed by hydrating the dried lipid films were freeze-thawed using liquid nitrogen and a water bath set at ~50 °C for five cycles. The solute-equilibrated MLVs obtained this way were extruded through polycarbonate filters (with a pore diameter of 100 nm) mounted in an extruder fitted with gastight Hamilton syringes. The final LUV suspension was prepared by subjecting the loaded samples to 19 passes through the polycarbonate filter. These LUVs were kept overnight in dark at room temperature (~23 °C) for equilibration before performing fluorescence measurements. In every case, a background sample (without DHE) was prepared following the same procedure.

Steady State Fluorescence Measurements

A Hitachi F-4010 spectrofluorometer (Tokyo, Japan) was employed for acquiring steady state fluorescence measurements at room temperature (~23 °C). Quartz cuvettes with 1 cm path length and excitation and emission slits with bandpass of 3 and 5 nm, respectively, were used for all measurements. Spectra were recorded in the corrected spectrum mode. Contributions from the solvent Raman peak and other scattering artifacts were cancelled out by subtracting intensities of background samples (without DHE) from each sample spectrum. Data shown is representative of

three independent measurements and the reported emission maxima in each case were identical (or within ± 1 nm of the values reported).

Membrane Depth Measurements by the Parallax Method

Fluorescence quenching of anthroyloxy-labeled fatty acids (2- and 12-AS) was utilized to estimate the actual spin (nitroxide) content of spin-labeled phospholipids (5- and 12-PC), as described previously [40]. Liposomes employed for depth measurements were prepared using 320 nmol of POPC containing 15 mol% spin-labeled phospholipid (5- or 12-PC) and 2 mol% DHE by the ethanol injection method, as described earlier [33]. The lipid and DHE mixture was co-dried to form dried lipid films, as described above for the preparation of LUVs for fluorescence measurements. Subsequently, the dried lipid film was dissolved in ethanol to ensure a final lipid concentration of 40 mM, which was then injected into the MOPS buffer (described above) while vortexing, to give a final lipid concentration of 213 μM. Duplicate samples were prepared in each case, except for background samples (without the quenchers, 5- or 12-PC) where triplicates were prepared. In addition, background samples (without DHE) were prepared for all sets of experiments, and their fluorescence intensity was subtracted from the respective sample fluorescence intensity. Samples were kept in the dark for 12 h at room temperature (~23 °C) for equilibration before fluorescence measurements.

Dipole Moment Calculations

Dipole moment calculations were carried out using a standard AM1 (Austin Model 1) program [41, 42], consisting of a modified MNDO Hamiltonian [43] and parametrized for polar systems and transition states. AM1 parametrization has proved to be an appropriate method for predicting the structure and energy properties of similar molecules, as evident from previous literature [44–50]. Importantly, it has been reported that the AM1 predictions are consistent with those obtained by other methods such as *ab initio* calculations with 6-31G* basis sets [47]. The calculations were carried out using the Hyperchem software (version 5.0 for Windows, Hypercube Inc., Canada).

Initial geometry optimization was achieved by MM+ molecular mechanics program, followed by unrestricted geometry optimization at the semiempirical level. The gradient norms were monitored to test for successful convergence. Excited state calculations were performed taking configuration interaction (CI) into account. The results presented were obtained with microstate CI calculation with the CI-active space made up of three highest occupied and three lowest unoccupied molecular orbitals.

Results and Discussion

Membrane penetration depth represents a relevant parameter in the context of membrane orientation of membrane-embedded molecules [51, 52]. Knowledge of the precise depth of a membrane-embedded group often helps define the conformation and topology of membrane probes and proteins. In addition, properties such as polarity, fluidity, segmental motion, ability to form hydrogen bonds, and extent of solvent penetration are known to vary in a depth-dependent manner in the membrane [53, 54]. To gain an overall understanding of the orientation and location of DHE in POPC membranes, we determined the penetration depth of the fluorescent moiety in DHE, utilizing the parallax method [55] using the equation:

$$Z_{cF} = L_{C1} + \left\{\left[(-1/\pi C)\ 1n\left(F_1/F_2\right) - L_{21}{}^2\right]/2\ L_{21}\right\} \quad (1)$$

where z_{cF} is the depth of the fluorophore from the center of the bilayer, L_{c1} is the distance of the center of the bilayer from the shallow quencher (5-PC in this case), L_{21} is the difference in depth between the two quenchers (*i.e.*, the transverse distance between the shallow and deep quenchers), and C is the two-dimensional quencher concentration in the plane of the membrane (molecules/Å^2). Here, F_1/F_2 is the ratio of F_1/F_o and F_2/F_o, in which F_1 and F_2 are the fluorescence intensities in the presence of the shallow quencher (5-PC) and the deep quencher (12-PC), respectively, both at the same quencher concentration C; and F_o is the fluorescence intensity in the absence of any quencher (for further details about these parameters, see ref [55]). Our results show that the depth of penetration of the fluorescent moiety of DHE, on the average, was ~12.8 Å from the center of the bilayer (see Table 1 and Fig. 2). This suggests that the fluorophore in DHE is localized at the interfacial region of the membrane. Interestingly, many fluorescent probes localized at the interfacial region of the membrane exhibit REES due to the unique physicochemical properties of this region [53].

REES is an excited state phenomenon observed with polar fluorophores in motionally restricted environments (such as

Table 1 Average membrane penetration depth of DHE in POPC membranes[a]

Spin-labeled PC pair utilized for quenching analysis	Calculated distance from the membrane bilayer center z_{cF} (Å)
5-PC/12-PC	~12.8

[a]Depth was calculated using Eq. (1), based on fluorescence quenching obtained with samples containing 15 mol% of 5-PC and 12-PC. Excitation and emission wavelengths of 326 and 373 nm, respectively, were used. DHE to lipid ratio was 1:50 (mol/mol) and DHE concentration was 4.27 μM in all cases. See Experimental for more details

Table 2 Dipole moments of DHE and cholesterol[a]

Compound	μ_g (D)	μ_e (D)	$\Delta\mu$ (D)
DHE	1.88	2.49	0.61
Cholesterol	1.92	2.03	0.11

[a]Calculated using the AM1 method. See Experimental and Fig. 5 for more details

membranes or proteins) [53, 56–59]. An important criterion for REES is that the time scale associated with solvent relaxation in the fluorophore microenvironment should be slower than or comparable to the fluorescence lifetime (~ns). This gives rise to the coupling of solvation dynamics to fluorophore local dynamics in the excited state. As a result, REES can be effectively utilized to monitor the organization and dynamics of fluorophores in restricted microenvironments. In operational terms, REES is defined as the shift in the emission maximum of a fluorophore toward longer wavelengths, due to a concomitant shift in the excitation wavelength toward the red edge of the absorption spectrum. Figure 3 shows fluorescence emission spectra of DHE in fluid phase POPC and gel phase DPPC vesicles with increasing excitation wavelength. A characteristic feature of the emission spectra is the maxima at 374 and 394 nm. Interestingly, the overall spectral shape remained invariant across the range of excitation wavelengths used (327, 337 and 347 nm), although there was a decrease in fluorescence intensity with increasing excitation wavelength. The reduction in intensity could be due to the photoselection of a smaller population of fluorophores at higher excitation wavelengths [53, 56]. To examine the effect of excitation wavelength on DHE fluorescence in more detail, we analyzed these fluorescence spectra in terms of the

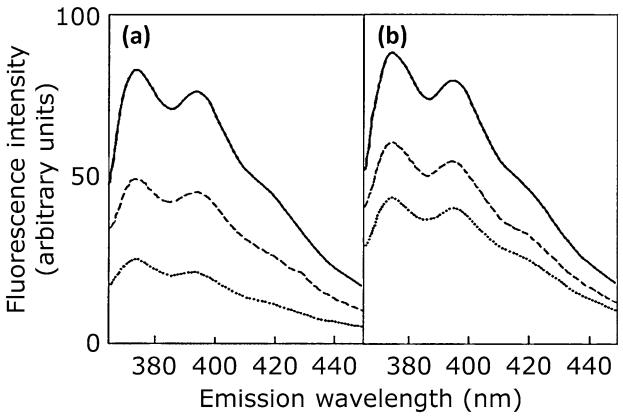

Fig. 3 (**a**) Representative fluorescence emission spectra of DHE with increasing excitation wavelength in (**a**) fluid phase POPC and (**b**) gel phase DPPC membranes. The spectra were acquired at excitation wavelengths of 327 nm (solid lines), 337 nm (dashed lines) and 347 nm (dotted lines). Data were recorded in the corrected spectrum mode. Concentrations of DHE and lipid were 11 and 213 μM, respectively. All experiments were carried out at room temperature (~23 °C). See Experimental for more details

dual emission maxima at 374 and 394 nm. Figure 4 depicts the effect of changing excitation wavelength on the emission maxima of DHE in fluid phase POPC and gel phase DPPC membranes. As seen from the figure, there was no change in the emission maxima (both peaks at 374 and 394 nm) as the excitation wavelength was increased from 327 to 357 nm. In other words, DHE does not exhibit any REES under these conditions. This is an intriguing observation, since DHE was found to be localized at the membrane interface (Table 1 and Fig. 2), an environment known to impose dynamic constraints on fluorophores [53], subsequently manifested as REES.

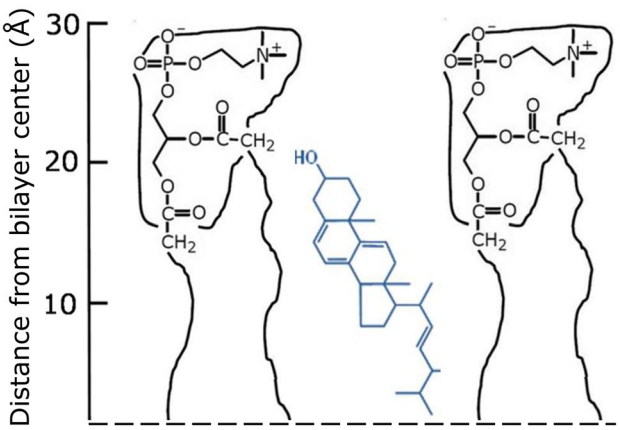

Fig. 2 Schematic representation of one-half of the membrane bilayer showing the membrane localization of DHE measured using the parallax method. The dotted line at the bottom represents the bilayer center. See text and Table 1 for more details

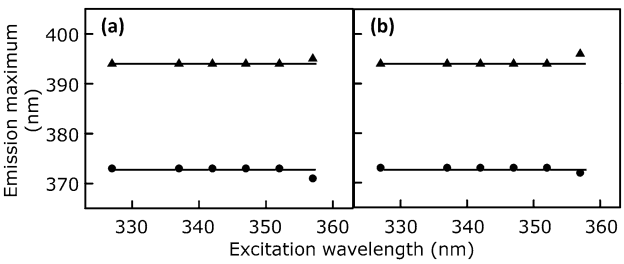

Fig. 4 Effect of changing excitation wavelength on emission maximum in (**a**) fluid phase POPC and (**b**) gel phase DPPC membranes, with emission monitored corresponding to two peaks shown in Fig. 3 (374 nm (circles) and 394 nm (triangles)). The invariance in fluorescence emission maxima upon changing excitation wavelength in all cases indicates lack of environmental sensitivity of DHE. Lines joining data points are provided merely as viewing guides. Concentrations of DHE and lipid were 11 and 213 μM, respectively. All experiments were carried out at room temperature (~23 °C). See Experimental for more details

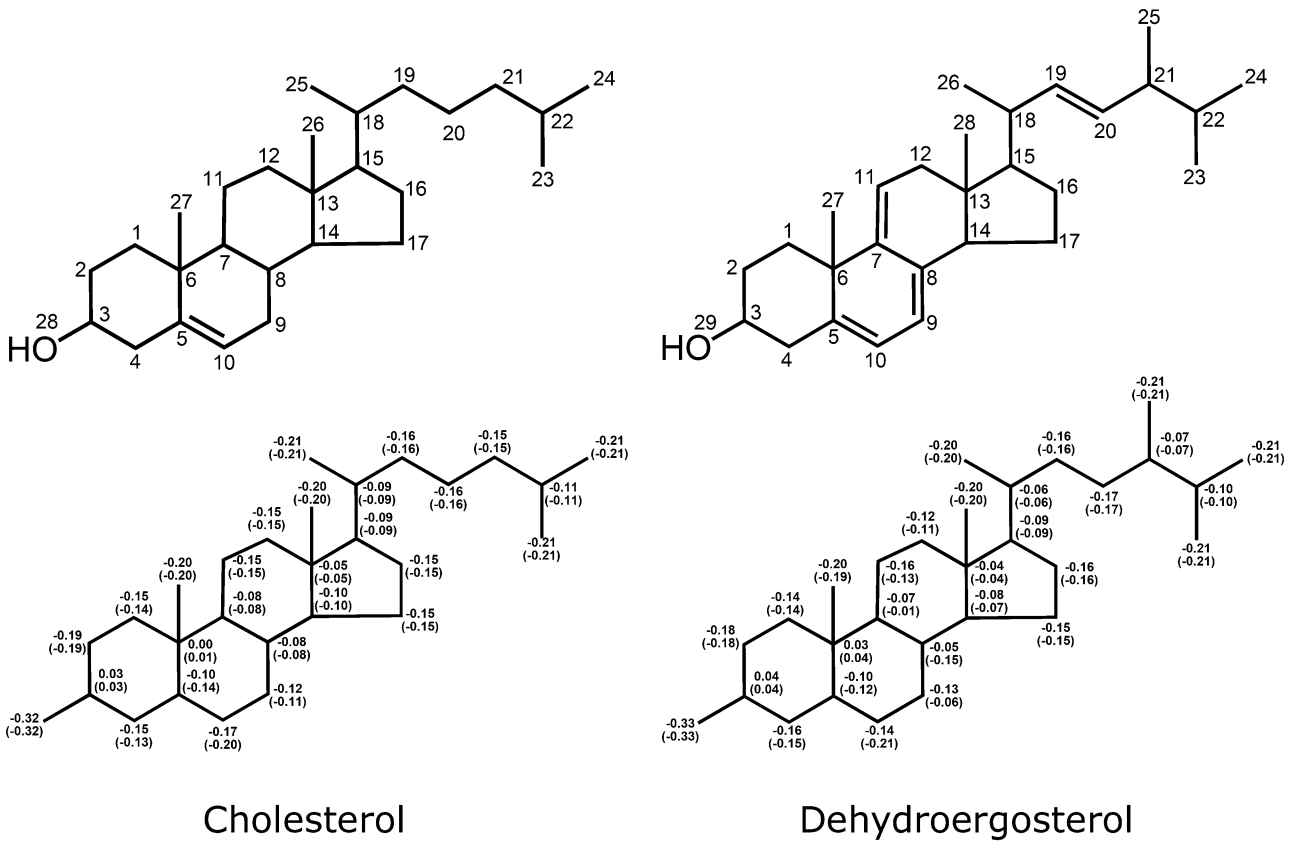

Fig. 5 Electronic charge densities at the ground and excited states for cholesterol (left) and dehydroergosterol (right), calculated using a standard AM1 program. Excited state charge densities are shown within parentheses. See Experimental and Table 2 for more details

An important requirement for REES is that the fluorophore should be polar, and more importantly, there should be an appreciable change in fluorophore dipole moment upon excitation [53, 56]. To explore this further, we determined the actual change in the dipole moment of DHE upon excitation using semi-empirical quantum chemical calculations [41, 42]. The electronic charge densities of DHE (and cholesterol as a control) in their ground and excited states, calculated using the AM1 program, are shown in Fig. 5. Dipole moments calculated from these charge densities and the differences in dipole moment between the ground and excited states (μ_g and μ_e) are shown in Table 2. The table shows that the difference in dipole moment ($\Delta\mu$) of DHE was rather modest (0.61 D). This essentially means that $\Delta\mu$ for DHE is too low to give rise to REES. We previously showed that phospholipids covalently labeled with the fluorescent NBD (7-nitrobenz-2-oxa-1,3-diazol-4-yl) group typically displays large REES [60, 61] due to a relatively large $\Delta\mu$ (~3.6 D) upon excitation [62].

Taken together, we report here that DHE, in spite of its localization at the membrane interface, fails to exhibit REES due to a very small change in its dipole moment upon excitation. Among the popular biologically useful fluorophores, probes such as NBD exhibit environmental sensitivity (solvatochromism) [63, 64]. NBD solvatochromism has previously been judiciously exploited to track the sorting pathway of a nascent secretory protein in the cellular milieu [65]. On the other hand, green fluorescent protein (GFP), the intrinsically fluorescent protein that revolutionized contemporary cell biological research [66, 67] has been shown to be insensitive to its environment [68, 69]. Our present results show that DHE represents yet another biologically relevant fluorophore that displays lack of environmental sensitivity, in spite of its popularity in monitoring cholesterol organization and traffic in model and biological membranes.

Acknowledgements This work was supported by intramural research grants from the Council of Scientific and Industrial Research, Govt. of India. A.C. gratefully acknowledges support from SERB Distinguished Fellowship (Department of Science and Technology, Govt. of India). S.C.B. thanks the Department of Biotechnology, Govt. of India, for the award of a Postdoctoral Fellowship. A.C. acknowledges help from Sreetama Pal and Parijat Sarkar during preparation of the manuscript. We thank members of the Chattopadhyay laboratory for their comments and discussions.

Authors' Contributions S.C.B. and R.R. performed experiments and analyzed data; S.S. carried out calculations under the supervision of

A.S.; A.C. conceptualized the project, designed experiments, wrote and edited the manuscript, organized access to research facilities and funding, and provided overall supervision and mentoring.

Funding This work was supported by intramural research grants from the Council of Scientific and Industrial Research, Govt. of India. A.C. gratefully acknowledges support from SERB Distinguished Fellowship (Department of Science and Technology, Govt. of India). S.C.B. thanks the Department of Biotechnology, Govt. of India, for the award of a Postdoctoral Fellowship.

Declarations

Disclosure of Potential Conflicts of Interest The authors declare that they have no conflict of interest.

References

1. Mouritsen OG, Zuckermann MJ (2004) What's so special about cholesterol? Lipids 39:1101–1113
2. Simons K, Ikonen E (2000) How cells handle cholesterol. Science 290:1721–1726
3. Kumar GA, Chattopadhyay A (2016) Cholesterol: an evergreen molecule in biology. Biomed Spectrosc Imaging 5:S55–S66
4. Mukherjee S, Maxfield FR (2004) Membrane domains. Annu Rev Cell Dev Biol 20:839–866
5. Chaudhuri A, Chattopadhyay A (2011) Transbilayer organization of membrane cholesterol at low concentrations: implications in health and disease. Biochim Biophys Acta 1808:19–25
6. Xu X, London E (2000) The effect of sterol structure on membrane lipid domains reveals how cholesterol can induce lipid domain formation. Biochemistry 39:843–849
7. Pucadyil TJ, Chattopadhyay A (2006) Role of cholesterol in the function and organization of G-protein coupled receptors. Prog Lipid Res 45:295–333
8. Barrantes FJ (2007) Cholesterol effects on nicotinic acetylcholine receptor. J Neurochem 103(Suppl 1):72–80
9. Paila YD, Chattopadhyay A (2010) Membrane cholesterol in the function and organization of G-protein coupled receptors. Subcell Biochem 51:439–466
10. Oates J, Watts A (2011) Uncovering the intimate relationship between lipids, cholesterol and GPCR activation. Curr Opin Struct Biol 21:802–807
11. Levitan I, Singh DK, Rosenhouse-Dantsker A (2014) Cholesterol binding to ion channels. Front Physiol 5:65
12. Sengupta D, Chattopadhyay A (2015) Molecular dynamics simulations of GPCR-cholesterol interaction: an emerging paradigm. Biochim Biophys Acta 1848:1775–1782
13. Gimpl G (2016) Interaction of G protein coupled receptors and cholesterol. Chem Phys Lipids 199:61–73
14. Jafurulla M, Kumar GA, Rao BD, Chattopadhyay A (2019) A critical analysis of molecular mechanisms underlying membrane cholesterol sensitivity of GPCRs. Adv Exp Med Biol 1115:21–52
15. Kumar GA, Jafurulla M, Chattopadhyay A (2016) The membrane as the gatekeeper of infection: cholesterol in host-pathogen interaction. Chem Phys Lipids 199:179–185
16. Subtil A, Gaidarov I, Kobylarz K, Lampson MA, Keen JH, McGraw TE (1999) Acute cholesterol depletion inhibits clathrin-coated pit budding. Proc Natl Acad Sci USA 96:6775–6780
17. Rodal SK, Skretting G, Garred Ø, Vilhardt F, van Deurs B, Sandvig K (1999) Extraction of cholesterol with methyl-β-cyclodextrin perturbs formation of clathrin-coated endocytic vesicles. Mol Biol Cell 10:961–974
18. Kumar GA, Chattopadhyay A (2020) Statin-induced chronic cholesterol depletion switches GPCR endocytosis and trafficking: insights from the serotonin$_{1A}$ receptor. ACS Chem Neurosci 11:453–465
19. Kumar GA, Chattopadhyay A (2021) Membrane cholesterol regulates endocytosis and trafficking of the serotonin$_{1A}$ receptor: insights from acute cholesterol depletion. Biochim Biophys Acta 1866:158882
20. Mukherjee S, Maxfield FR (1999) Cholesterol: stuck in traffic. Nat Cell Biol 1:E37–E38
21. Schroeder F (1984) Fluorescent sterols: probe molecules of membrane structure and function. Prog Lipid Res 23:97–113
22. Wüstner D (2007) Fluorescent sterols as tools in membrane biophysics and cell biology. Chem Phys Lipids 146:1–25
23. Gimpl G, Gehrig-Burger K (2007) Cholesterol reporter molecules. Biosci Rep 27:335–358
24. Gimpl G, Gehrig-Burger K (2011) Probes for studying cholesterol binding and cell biology. Steroids 76:216–231
25. Schroeder F, Jefferson JR, Kier AB, Knittel J, Scallen TJ, Wood WG, Hapala I (1991) Membrane cholesterol dynamics: cholesterol domains and kinetic pools. Proc Soc Exp Biol Med 196:235–252
26. Schroeder F, Woodford JK, Kavecansky J, Wood WG, Joiner C (1995) Cholesterol domains in biological membranes. Mol Membr Biol 12:113–119
27. Mukherjee S, Zha X, Tabas I, Maxfield FR (1998) Cholesterol distribution in living cells: fluorescence imaging using dehydroergosterol as a fluorescent cholesterol analog. Biophys J 75:1915–1925
28. Robalo JR, do Canto AMTM, Carvalho AJP, Ramalho JPP, Loura LMS (2013) Behavior of fluorescent cholesterol analogues dehydroergosterol and cholestatrienol in lipid bilayers: a molecular dynamics study. J Phys Chem B 117:5806–5819
29. Pourmousa M, Róg T, Mikkeli R, Vattulainen I, Solanko LM, Wüstner D, List DH, Kongsted J, Karttunen M (2014) Dehydroergosterol as an analogue for cholesterol: why it mimics cholesterol so well — or does it? J Phys Chem B 118:7345–7357
30. Frolov A, Petrescu A, Atshaves BP, So PTC, Gratton E, Serrero G, Schroeder F (2000) High density lipoprotein-mediated cholesterol uptake and targeting to lipid droplets in intact L-cell fibroblasts. A single- and multiphoton fluorescence approach. J Biol Chem 275:12769–12780
31. Matyash V, Geier C, Henske A, Mukherjee S, Hirsh D, Thiele C, Grant B, Maxfield FR, Kurzchalia TV (2001) Distribution and transport of cholesterol in *Caenorhabditis elegans*. Mol Biol Cell 12:1725–1736
32. Rukmini R, Rawat SS, Biswas SC, Chattopadhyay A (2001) Cholesterol organization in membranes at low concentrations: effects of curvature stress and membrane thickness. Biophys J 81:2122–2134
33. Raghuraman H, Chattopadhyay A (2004) Interaction of melittin with membrane cholesterol: a fluorescence approach. Biophys J 87:2419–2432
34. Maxfield FR, Wüstner D (2012) Analysis of cholesterol trafficking with fluorescent probes. Methods Cell Biol 108:367–393
35. Eftink MR (1991) Fluorescence techniques for studying protein structure. In: Suelter CH (ed) Methods of biochemical analysis. John Wiley, New York, vol 35, pp 127–205
36. Chattopadhyay A, Rukmini R, Mukherjee S (1996) Photophysics of a neurotransmitter: ionization and spectroscopic properties of serotonin. Biophys J 71:1952–1960
37. Smutzer G, Crawford BF, Yeagle PL (1986) Physical properties of the fluorescent sterol probe dehydroergosterol. Biochim Biophys Acta 862:361–371

38. Dittmer JC, Lester RL (1964) A simple, specific spray for the detection of phospholipids on thin-layer chromatograms. J Lipid Res 5:126–127
39. McClare CWF (1971) An accurate and convenient organic phosphorus assay. Anal Biochem 39:527–530
40. Abrams FS, London E (1993) Extension of the parallax analysis of membrane penetration depth to the polar region of model membranes: use of fluorescence quenching by a spin-label attached to the phospholipid polar headgroup. Biochemistry 32:10826–10831
41. Dewar MJS, Zoebisch EG, Healy EF, Stewart JJP (1985) Development and use of quantum mechanical molecular models. 76. AM1: a new general purpose quantum mechanical molecular model. J Am Chem Soc 107:3902–3909
42. Dewar MJS, Dieter KM (1986) Evaluation of AM1 calculated proton affinities and deprotonation enthalpies. J Am Chem Soc 108:8075–8086
43. Dewar MJS, Thiel W (1977) Ground states of molecules. 38. The MNDO method. Approximations and parameters. J Am Chem Soc 99:4899–4907
44. McCarthy PK, Blanchard GJ (1993) AM1 study of the electronic structure of coumarins. J Phys Chem 97:12205–12209
45. Awad MM, McCarthy PK, Blanchard GJ (1994) Photoisomerization of cyanines. A comparative study of oxygen- and sulfur-containing species. J Phys Chem 98:1454–1458
46. Gorse A-D, Pesquer M (1993) A theoretical study of aniline and some derivatives in their ground states. J Mol Struc-Theochem 281:21–32
47. Gorse A-D, Pesquer M (1995) Intramolecular charge transfer excited state relaxation processes in para-substituted N, N-dimethylaniline: a theoretical study including solvent effects. J Phys Chem 99:4039–4049
48. Soujanya T, Saroja G, Samanta A (1995) AM1 study of the twisted intramolecular charge transfer phenomenon in *p*-(N, N-dimethylamino)benzonitrile. Chem Phys Lett 236:503–509
49. Soujanya T, Fessenden RW, Samanta A (1996) Role of nonfluorescent twisted intramolecular charge transfer state on the photophysical behavior of aminophthalimide dyes. J Phys Chem 100:3507–3512
50. Saroja G, Sankaran NB, Samanta A (1996) Photophysical study of two carbostyril dyes: investigation of the possible role of a rotary decay mechanism. Chem Phys Lett 249:392–398
51. Chattopadhyay A (1992) Membrane penetration depth analysis using fluorescence quenching: a critical review. In: Gaber BP, Easwaran KRK (eds) Biomembrane structure and function: the state of the art. Adenine Press, Schenectady, NY, pp 153–163
52. London E, Ladokhin AS (2002) Measuring the depth of amino acid residues in membrane-inserted peptides by fluorescence quenching. In: Benos D, Simon S (eds) Current topics in membranes. Elsevier, San Diego, pp 89–115
53. Haldar S, Chaudhuri A, Chattopadhyay A (2011) Organization and dynamics of membrane probes and proteins utilizing the red edge excitation shift. J Phys Chem B 115:5693–5706
54. Pal S, Chattopadhyay A (2017) What is so unique about biomembrane organization and dynamics ? In: Chattopadhyay A (ed) Membrane organization and dynamics. Springer, Heidelberg, pp 1–9
55. Chattopadhyay A, London E (1987) Parallax method for direct measurement of membrane penetration depth utilizing fluorescence quenching by spin-labeled phospholipids. Biochemistry 26:39–45
56. Mukherjee S, Chattopadhyay A (1995) Wavelength-selective fluorescence as a novel tool to study organization and dynamics in complex biological systems. J Fluoresc 5:237–246
57. Demchenko AP (2008) Site-selective red-edge effects. Methods Enzymol 450:59–78
58. Chattopadhyay A, Haldar S (2014) Dynamic insight into protein structure utilizing red edge excitation shift. Acc Chem Res 47:12–19
59. Brahma R, Raghuraman H (2021) Novel insights in linking solvent relaxation dynamics and protein conformations utilizing red edge excitation shift approach. Emerg Top Life Sci 5:89-101
60. Chattopadhyay A, Mukherjee S (1993) Fluorophore environments in membrane-bound probes: a red edge excitation shift study. Biochemistry 32:3804–3811
61. Mukherjee S, Raghuraman H, Dasgupta S, Chattopadhyay A (2004) Organization and dynamics of *N*-(7-nitrobenz-2-oxa-1,3-diazol-4-yl)-labeled lipids: a fluorescence approach. Chem Phys Lipids 127:91–101
62. Mukherjee S, Chattopadhyay A, Samanta A, Soujanya T (1994) Dipole moment change of NBD group upon excitation studied using solvatochromic and quantum chemical approaches: implications in membrane research. J Phys Chem 98:2809–2812
63. Chattopadhyay A (1990) Chemistry and biology of *N*-(7-nitrobenz-2-oxa-1,3-diazol-4-yl)-labeled lipids: fluorescence probes of biological and model membranes. Chem Phys Lipids 53:1–15
64. Haldar S, Chattopadhyay A (2013) Application of NBD-labeled lipids in membrane and cell biology. In: Mely Y, Duportail G (eds), Springer Series on Fluorescence. Springer, Heidelberg, vol. 13, pp 37–50
65. Crowley KS, Reinhart GD, Johnson AE (1993) The signal sequence moves through a ribosomal tunnel into a noncytoplasmic aqueous environment at the ER membrane early in translocation. Cell 73:1101–1115
66. Haldar S, Chattopadhyay A (2009) Green fluorescent protein: a molecular lantern that illuminates the cellular interior. J Biosci 34:169–172
67. Tsien RY (2009) Constructing and exploiting the fluorescent protein paintbox (Nobel lecture). Angew Chem Int Ed 48:5612–5626
68. Haldar S, Chattopadhyay A (2007) Dipolar relaxation within the protein matrix of the green fluorescent protein: a red edge excitation shift study. J Phys Chem B 111:14436–14439
69. Sarkar P, Chattopadhyay A (2018) GFP fluorescence: a few lesser-known nuggets that make it work. J Biosci 43:421–430